# A novel norindenoisoquinoline structure reveals a common interfacial inhibitor paradigm for ternary trapping of the topoisomerase I-DNA covalent complex

**Christophe Marchand,[1] Smitha Antony,[1] Kurt W. Kohn,[1] Mark Cushman,[2] Alexandra Ioanoviciu,[2] Bart L. Staker,[3] Alex B. Burgin,[3] Lance Stewart,[3] and Yves Pommier[1]**

[1]Laboratory of Molecular Pharmacology, Center for Cancer Research, National Cancer Institute, Bethesda, Maryland; [2]Department of Medicinal Chemistry and Molecular Pharmacology and the Purdue Cancer Center, School of Pharmacy and Pharmaceutical Sciences, Purdue University, West Lafayette, Indiana; and [3]deCODE Biostructures, Inc., Bainbridge Island, Washington

## Abstract

**We show that five topoisomerase I inhibitors (two indenoisoquinolines, two camptothecins, and one indolocarbazole) each intercalate between the base pairs flanking the cleavage site generated during the topoisomerase I catalytic cycle and are further stabilized by a network of hydrogen bonds with topoisomerase I. The interfacial inhibition paradigm described for topoisomerase I inhibitors can be generalized to a variety of natural products that trap macromolecular complexes as they undergo catalytic conformational changes that create hotspots for drug binding. Stabilization of such conformational states results in uncompetitive inhibition and exemplifies the relevance of screening for ligands and drugs that stabilize (''trap'') these macromolecular complexes. [Mol Cancer Ther 2006;5(2):287–95]**

## Introduction

DNA topoisomerase I, an essential enzyme in metazoans (1, 2), has been identified as the target of camptothecin and its derivatives (3, 4). Topoisomerase I is ubiquitous and highly conserved in eukaryotes (5–7). The enzymatic activity of topoisomerase I, like that of other topoisomerases, breaks the DNA backbone reversibly by replacing a DNA phosphodiester bond with a bond between a phosphate at one end of the DNA break and a tyrosine residue of the topoisomerase I protein. In the case of topoisomerase I, the tyrosine links to the phosphate at the 3′-hydroxyl end of the DNA break (Fig. 1A-C). DNA relaxation takes place by rotation of the free end of the broken DNA around the intact DNA strand (Fig. 1B; ref. 8).

Camptothecin was discovered as the active principle of extracts from the Chinese tree *Camptotheca acuminata* by Wall and Wani (9). Camptothecin is a planar heterocycle consisting of five rings, including an important α-hydroxylactone E-ring (Fig. 1F). Camptothecin has several remarkable features. First, the natural alkaloid is the 20S-camptothecin enantiomer; this is the form that is active against topoisomerase I and experimental cancers, whereas the synthetic 20R enantiomer lacks both activities (9). Second, camptothecin traps the topoisomerase I-DNA cleavage complex, forming a potentially lethal DNA lesion. The anticancer activity thus is not due to inhibition of the topoisomerase I enzyme activity per se. This distinction was shown in topoisomerase I–deficient yeast strains, which completely lack the camptothecin sensitivity of wild-type strains (10–12). Third, camptothecin does not bind significantly to either DNA or purified topoisomerase I: both must be present together in the form of cleavage complexes (9). These characteristics led to the hypothesis that camptothecin forms a ternary complex with topoisomerase I and its DNA substrate by binding to a stereospecific site in the topoisomerase I-DNA cleavage complex (Fig. 1C; ref. 13). The DNA sequence at the cleavage sites has a strong bias for a guanine residue at the 5′ side of the DNA break (14). In view of the aromatic planar structure of camptothecin resembling a fused DNA base pair, it was hypothesized that camptothecin forms a ternary complex with topoisomerase I and DNA, stacking against a guanine-containing base pair on the 5′ side of the break while at the same time binding to sites on the topoisomerase I protein (14). Camptothecin thus is stabilized at a topoisomerase I-DNA interface in a structure similar to a normal intermediate in the topoisomerase reaction (Fig. 1C). By convention, the base pairs flanking the break are called −1 and +1. Position −1 corresponds to the nucleotide covalently linked to topoisomerase I and +1 to the nucleotide at the free 5′-hydroxyl terminus (Fig. 1A-C). The atomic structure of a ternary topoisomerase I cleavage complex was revealed by X-ray crystallography with the clinical camptothecin derivative topotecan (see structure in Fig. 1F). This structure

Received 11/3/05; accepted 12/16/05.

**Grant support:** Intramural Research Program of the NIH, National Cancer Institute, Center for Cancer Research, and NIH Grant U01 CA89566.

The costs of publication of this article were defrayed in part by the payment of page charges. This article must therefore be hereby marked advertisement in accordance with 18 U.S.C. Section 1734 solely to indicate this fact.

**Requests for reprints:** Yves Pommier, Laboratory of Molecular Pharmacology, Center for Cancer Research, National Cancer Institute, Building 37, Room 5068, Bethesda, MD 20892-4255. Phone: 301-496-5944; Fax: 301-402-0752. E-mail: pommier@nih.gov



doi:10.1158/1535-7163.MCT-05-0456

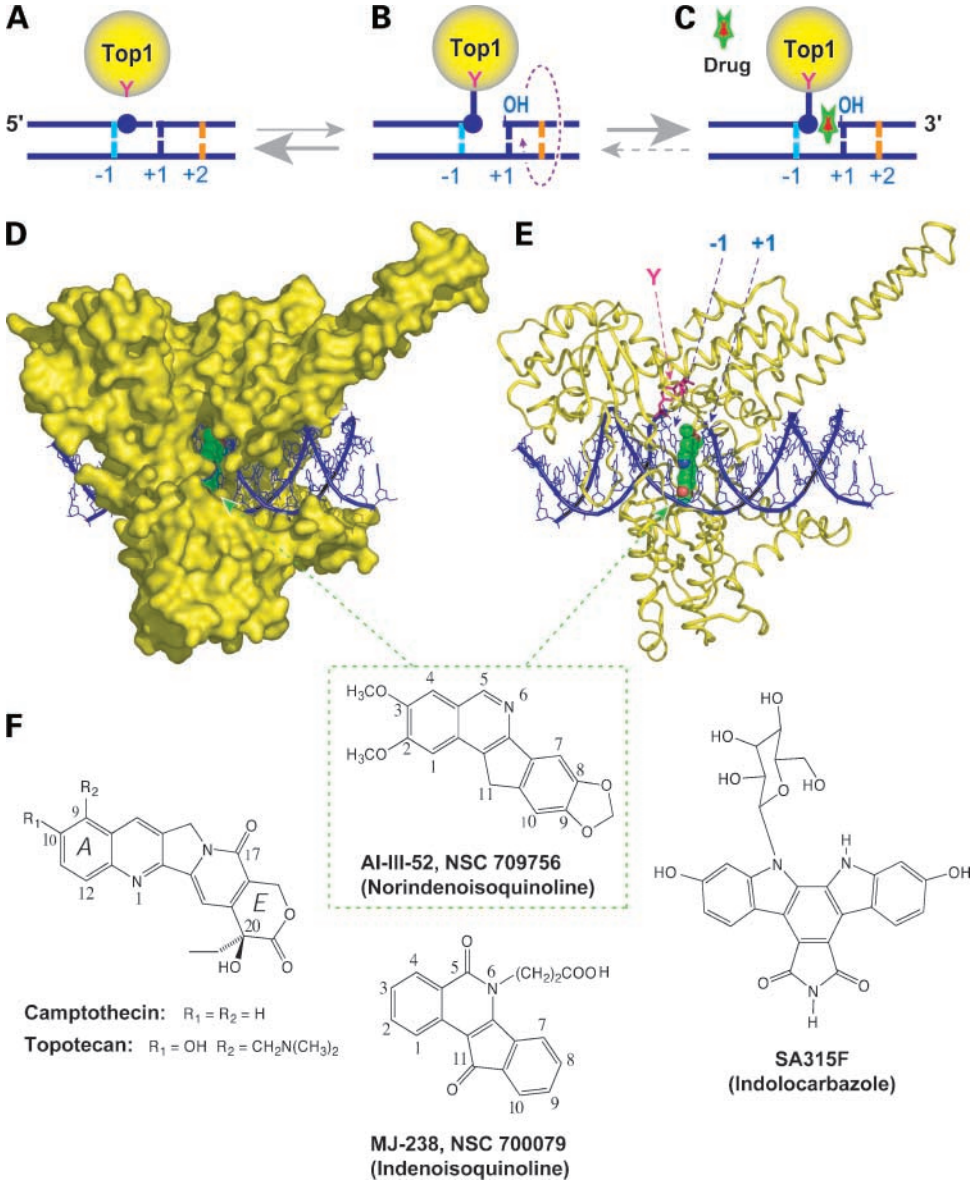


**Figure 1.** Structure of the topoisomerase I cleavage complex trapped by the norindenoisoquinoline AI-III-52. **A** and **B,** topoisomerase I (*Top1*) nicking-closing reaction. **A,** topoisomerase I is generally bound noncovalently to DNA. *Red* (*Y*), topoisomerase I catalytic tyrosine (Y723 for human nuclear topoisomerase I). **A** to **B,** topoisomerase I cleaves one strand of the duplex as it forms a covalent phosphodiester bond between the catalytic tyrosine and the 3′ DNA terminus. The other DNA terminus is a 5′-hydroxyl (*OH*). **B,** topoisomerase I cleavage complex allows rotation of the 5′ terminus around the intact strand, which relaxes DNA supercoiling (*purple dotted circle with arrowhead*). **B** to **A,** following DNA relaxation, topoisomerase I religates the DNA. Under normal conditions, the religation (closing) reaction rate constant is much higher than the cleavage (nicking) rate constant. More than 90% of the topoisomerase I-DNA complexes are noncovalent (as in **A**). **C,** each of the topoisomerase I inhibitors in **F** traps the topoisomerase I cleavage complex by binding at the enzyme-DNA interface between the base pairs flanking the topoisomerase I–mediated DNA cleavage site (by convention positions −1 and +1). The colors for the bp −1 (*light blue*), +1 (*dark blue*), and +2 (*orange*) are the same as in Fig. 3. **D** and **E,** lateral views of a topoisomerase I-DNA complex trapped by the norindenoisoquinoline AI-III-52 (*green* and *red*). **D,** topoisomerase I (*yellow*) is shown in a surface view to represent the depth of the norindenoisoquinoline binding pocket. **E,** topoisomerase I is represented in ribbon diagram to allow visualization of the catalytic tyrosine (*Y*; *red*) and to show the drug intercalation between the −1 and +1 bp. **F,** chemical structure of the five drugs cocrystallized with topoisomerase I-DNA complexes (15, 16, 24).

confirmed the drug-stacking hypothesis (15). More recently, we found the binding of the natural camptothecin alkaloid to the topoisomerase I-DNA complex to be remarkably similar to the topotecan structure (16).

Because of the anticancer activity of camptothecins, many derivatives have been synthesized for clinical development (17). Two of these have been approved by the U.S. Food and Drug Administration: topotecan (Hycamtin) for ovarian and lung cancers and irinotecan (CPT11; Campto) for colon carcinomas. Several other derivatives are in preclinical development or clinical trial (Exatecan, 9-nitrocamptothecin, BAY 38-3441; refs. 18, 19). Camptothecins, however,

have limitations. The α-hydroxylactone in the E-ring (see Fig. 1F) is rapidly converted in the circulation to a carboxylate whose tight binding to serum albumin limits the available active drug (20). In addition, camptothecins are actively exported from the cell by drug efflux membrane ''pumps'' (21).

Non-camptothecin topoisomerase I inhibitors are therefore of great pharmaceutical interest to overcome the limitations of camptothecins. Moreover, because drugs from different chemical families that share the same molecular target generally have different spectra of clinical activity, non-camptothecin topoisomerase I inhibitors may be effective against different tumors. For instance, this is the case for the tubulin and the topoisomerase II inhibitors (17). Indenoisoquinoline and indolocarbazole derivatives (Fig. 1F) are being pursued for therapeutic development. The first indenoisoquinoline topoisomerase I inhibitor was discovered by searching the National Cancer Institute cell screen database for compounds resembling camptothecin in their cytotoxicity profile against 60 human cancer cell lines (22). In the absence of definitive structural information of the drug target site, derivatives were initially designed with amino groups that would bind electrostatically to the polyanionic phosphodiester backbone. Over 300 indenoisoquinoline derivatives have been synthesized to date, and several potent and selective topoisomerase I inhibitors have been identified as potential anticancer agents (17, 23). We recently reported the first crystal structure of an indenoisoquinoline (MJ-238; Fig. 1F) bound to a topoisomerase I cleavage complex (16). In the same study, we also reported the structure of the natural camptothecin alkaloid and of an indolocarbazole (SA315F; Fig. 1F) bound to the topoisomerase I-DNA complex (16).

This study describes the crystal structure of a potent norindenoisoquinoline (24), topoisomerase I inhibitor (AI-III-52), in a complex with DNA and topoisomerase I. Comparison with the corresponding ternary complexes of the MJ-238 indenoisoquinoline (16) and with the structures of camptothecin (16), topotecan (15), and an indolocarbazole (16) reveals a common molecular mechanism of drug action. These topoisomerase I inhibitors all bind at the topoisomerase I-DNA interface by intercalating and stacking between the base pairs flanking the DNA cleavage site and by forming critical hydrogen bonds with topoisomerase I amino acid residues. These same topoisomerase I residues have been implicated previously in enzyme catalysis and/or resistance to camptothecins (25). We discuss topoisomerase I inhibitors as paradigms for drugs that trap macromolecular interfaces and the generality and implications of the interfacial inhibitor concept (26, 27).

## Materials and Methods

A 70-kDa construct of human topoisomerase I (topoisomerase 70), residues $Lys^{175}$ to $Phe^{765}$, was expressed and purified from baculovirus insect cells (Sf9) as described previously (28). Crystallization trials were conducted with wild-type topoisomerase 70 and duplex DNA oligomers containing a 5′ bridging phosphorothiolate linkage at the site of DNA cleavage (15, 16). Crystals were grown by sitting drop vapor diffusion by preparing drops containing 2 mL precipitant, 1.5 mL of 50 mmol/L duplex DNA, 0.5 mL compound, and 1.5 mL of 4.2 mg/mL protein. Precipitant was 10% to 12% polyethylene glycol 8000, 100 mmol/L MES (pH 6.4), and 200 mmol/L lithium sulfate. The compound solutions used were 1 to 5 mmol/L ligand dissolved in DMSO (0–10%, v/v) in water. Crystals were cryoprotected for data collection by passing them through precipitant plus 30% (v/v) polyethylene glycol 400. Data were collected at 100 K at Beamline 5.0.3 (Advanced Light Source, Lawrence Berkeley National Laboratory, Berkeley, CA). Structures were solved by molecular replacement using the program AMORE (29) with protein coordinates from the topoisomerase 70 ternary complex structure with topotecan (15). Refinements were conducted using CNX (30) and REFMAC (31) and iterative model adjustments with XtalView (see Table 1; ref. 32). DNAs were placed into the |Fo| − |Fc| electron density and refined. Drug molecules were then placed into the to |Fo| − |Fc| electron density using QUANTA module X-LIGAND (33). The diffraction resolution of the crystals obtained was 3.1 Å and this did not allow the placement of water molecules.

Molecular visualization was done using PyMOL. The PDB codes for the different topoisomerase I crystal structures were 1LT8 for norindenoisoquinoline (24), 1SC7 for MJ-238 (16), 1SEU for indolocarbazole (16), 1K4T for topotecan (15), 1T81 for camptothecin (16), and 1A31 for topoisomerase I in the absence of inhibitor (34).

**Table 1. Refinement statistics**

| | |
|---|---|
| Inhibitor bound | AI-III-52 |
| PDBID | 1TL8 |
| Resolution (Å) | 50–3.1 (3.21–3.10) |
| No. reflections | 16,738 (1,581) |
| $R_{sym}$ | 10.0 (52.2) |
| Completeness | 97.8 (93.1) |
| $I/\sigma I$ | 13.7 (2.3) |
| Space group | P21 |
| *a* (Å) | 56.949 |
| *b* (Å) | 114.140 |
| *c* (Å) | 73.499 |
| *β* | 94.18 |
| Reflections used in RFREE | 5%, 808 |
| No. protein atoms | 4,703 |
| No. DNA atoms | 892 |
| No. inhibitor atoms | 24 |
| No. solvent atoms | 0 |
| RFACTOR | 22.9 (33.2) |
| RFREE | 30.5 (39.5) |
| r.m.s. deviations from ideal stereochemistry | |
| Bond lengths (Å) | 0.017 |
| Bond angles (°) | 1.9 |
| Impropers (°) | 3.94 |
| Dihedrals (°) | 23.8 |
| Mean B factor; all atoms (Å$^3$) | 60.4 |

NOTE: $R_{sym} = \Sigma|I_i - I_m| / \Sigma I_m$, where $I_i$ is the intensity of the measured reflection and $I_m$ is the mean intensity of all symmetry related reflections. Numbers in parentheses represent final shell of data.

## Results and Discussion

### Norindenoisoquinoline AI-III-52 Intercalates between the Base Pairs Flanking the Topoisomerase I – Mediated DNA Break

The overall structure the AI-III-52 norindenoisoquinoline in a topoisomerase I cleavage complex is presented in Fig. 1D and E. The drug is bound deep inside topoisomerase I (Fig. 1D), intercalated between the base pairs flanking the DNA cleavage site (positions −1 and +1; Fig. 1E). The topoisomerase I protein encircles the DNA in a closed clamp conformation (34–36). The polypeptide hinge is behind the DNA, and the tight narrow cleft through which the DNA has presumably entered the enzyme is represented in front of the DNA. The topoisomerase I enzyme used in these experiments comprises the core, linker, and catalytic domain. It does not include the topoisomerase I $NH_2$-terminal domain that encompasses residues 1 to 174 and that is not well conserved among eukaryotic topoisomerase I enzymes. The $NH_2$ terminus has been shown both *in vitro* and *in vivo* to be dispensable with respect to the biochemical and cytotoxic effects of topoisomerase I poisons, including camptothecin and topotecan (28, 37). Technical aspects of structure determination are summarized in Table 1.

Figure 2A shows two expanded views of AI-III-52 bound to the DNA in the topoisomerase I cleavage complex. Fig. 2A (*left*) is in the same view orientation as Fig. 1D and E, with the DNA cleavage site seen from the minor groove. Fig. 2A (*right*) is a 90° rotation showing AI-III-52 under the +1 nucleotide pair. The +1 bp (shown as capped sticks) covers and stacks against the entire drug (shown in space filling model). Extensive stacking is also the case for the −1 bp, which is completely covered by the drug and therefore not shown in Fig. 2A (*right*). Figure 3B shows the relative positions of the base pairs flanking the intercalated norindenoisoquinoline molecule. The +1 bp is oriented as in Fig. 2A (*right*), and the drug molecule is not shown. The longitudinal axes of the +1 and −1 bp (shown as thin dashed lines) are almost parallel. Thus, the twist angle between the base pairs flanking the intercalated drug is reduced to 10°.

DNA unwinding is a characteristic of DNA intercalators, caused by the increased distance between flanking base pairs required to accommodate the intercalated molecule. For instance, intercalation of ethidium reduces the twist angle between the flanking bases pairs to 7° compared with the normal 33°. The reduction in the twist angle between

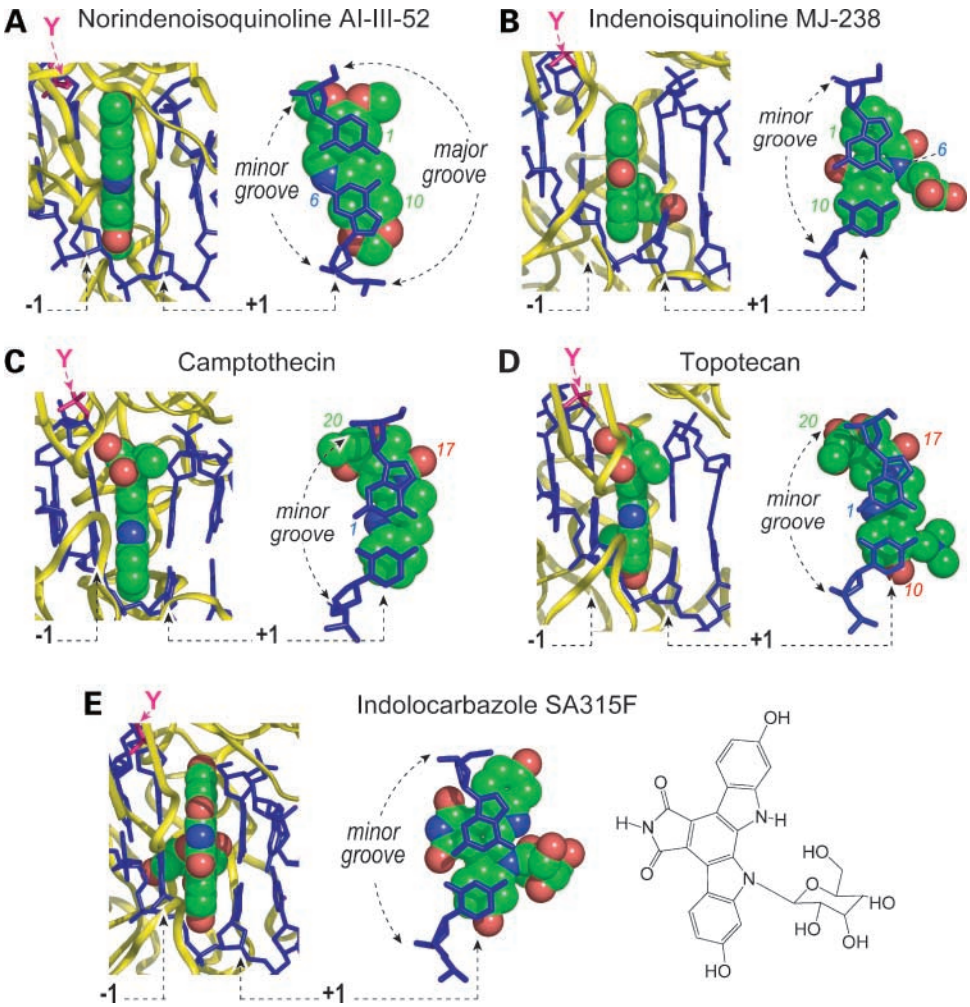


**Figure 2.** Stacking of a drug molecule between two base pairs flanking the topoisomerase I cleavage complex is a common mechanism for the indenoisoquinolines (**A** and **B**), the camptothecins (**C** and **D**), and an indolocarbazole derivative (**E**). Each panel shows two views for each drug within the topoisomerase I cleavage complex. *Left,* oriented as in Fig. 1D and E, with the DNA viewed from the minor groove; *right,* rotated 90° and showing the +1 nucleotides covering the drug molecules. The catalytic topoisomerase I tyrosine is shown in red (*Y*) at the top left of each panel. *Dashed arrows,* −1 and +1 bp. Colored numbers correspond to the drug atoms numbered in Fig. 4. The orientation of SA315F is the same in the middle and right in **E**.

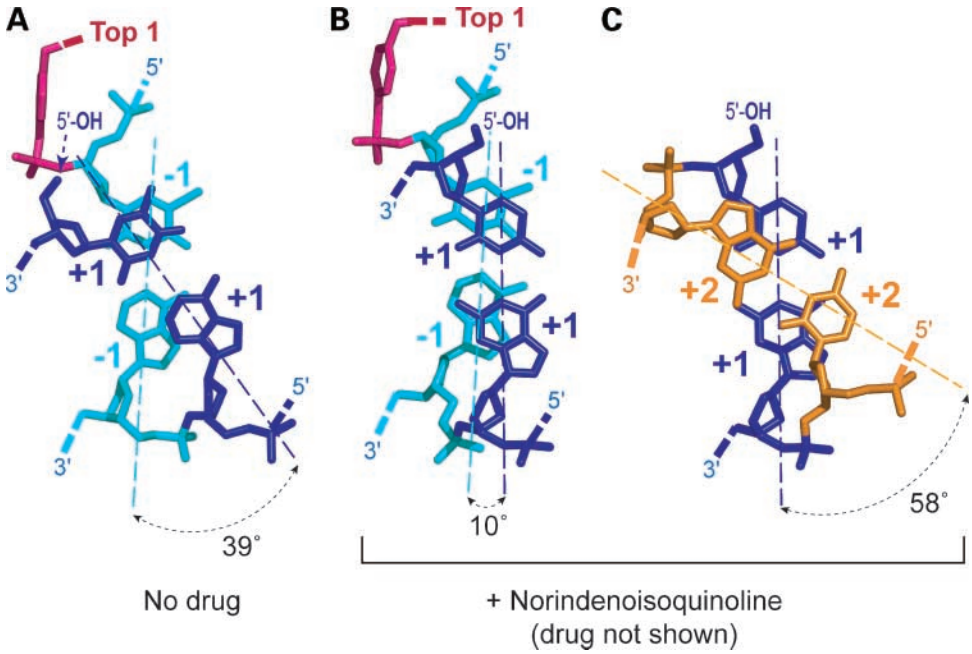


**Figure 3.** DNA unwinding by the norindenoisoquinoline AI-III-52. **A,** twist angle between the base pairs flanking the topoisomerase I cleavage site in the absence of inhibitor (34). *Thin dashed lines,* base pair long axes; *dark blue,* +1 bp; *cyan,* −1 bp. **B,** twist angle between the base pairs flanking the topoisomerase I cleavage site trapped by AI-III-52. The drug has been removed to only show the −1 and +1 nucleotides. The +1 nucleotides are positioned similarly to **A**. *Thin dashed lines,* base pair long axes. **C,** twist angle between the +1 and +2 bp. The color code is the same as in Fig. 1A to C.

flanking base pairs for the norindenoisoquinoline AI-III-52 intercalated in the topoisomerase I-DNA cleavage complex (Fig. 3B) is comparable with that produced by intercalated ethidium. The twist angle reduction observed with AI-III-52 is not due to topoisomerase I cleavage, because the twist angle between the base pair flanking the topoisomerase I cleavage site in the absence of drug remains near normal (Fig. 3A; ref. 34). The twist angle of 58° between +1 and +2 bp in the norindenoisoquinoline structure indicates slight overwinding of the DNA immediately adjacent to the drug binding (Fig. 3C). This overwinding probably compensates for the unwinding produced by the norindenoisoquinoline.

**Camptothecin, Topotecan, MJ-238, and Indolocarbazole Also Intercalate between the Base Pairs Flanking the Topoisomerase I – Mediated DNA Break**

Figure 2B shows that the indenoisoquinoline MJ-238 (see structure in Fig. 1F), like the norindenoisoquinoline AI-III-52, stacks and intercalates between bp −1 and +1 on each side of the cleavage site generated by topoisomerase I. For both drugs, their aromatic portion is parallel to the −1 and +1 bp long axes. However, the two indenoisoquinolines are flipped 180° (Figs. 2 and 4, compare A and B). Numbering of the corresponding atoms makes this difference apparent. For AI-III-52, the sequence of atoms in a clockwise orientation is *1, 10*, and *6*, whereas for MJ-238 the sequence is *1, 6*, and *10*. In other words, AI-III-52 is intercalated with the nitrogen *N6* in the minor groove. This nitrogen *N6* can hydrogen bond with the topoisomerase I R364 residue. By contrast, MJ-238 has the nitrogen *N6* in the major groove of the DNA and the *C11* carbonyl hydrogen bonded to R364. The side chain attached to the nitrogen *N6* protrudes in the DNA major groove (Fig. 2B).

Like the indenoisoquinolines, the two camptothecins intercalate between −1 and +1 bp at the cleavage site of the topoisomerase I-DNA complex (Fig. 2C and D; refs. 15, 16). Both camptothecins stack in the same orientation. Their five-membered planar heterocyclic structure coincides with the long axis of the base pairs, and their shapes closely match that of a base pair. The hydroxyl substituents at the 20-position are in close proximity with the sugar of the −1 nucleotide and the DNA phosphodiester backbone and contribute to the optimum stacking of the natural 20S-camptothecin enantiomer. This explains why the 20R-camptothecin enantiomer cannot trap the topoisomerase I catalytic complex (13). At the other end of the camptothecin, the A ring is not immediately in contact with the DNA phosphodiester backbone opposite from the cleavage site. This space can accommodate the 10-hydroxy substituent of topotecan. Filling this space probably accounts for the greater potency of 10-hydroxy-substituted camptothecins and for the even greater activity of 10,11-dimethoxy-camptothecin derivatives (13, 38).

The indolocarbazole SA315F is also bound with maximum stacking interactions. The indolocarbazole aromatic portion is aligned with the axis of the −1 and +1 bp (Fig. 2E; ref. 16). The deoxyribose is positioned in the major groove.

For the indenoisoquinoline MJ-238, topotecan, and the indolocarbazole SA315F, the drug aromatic polycyclic ring is parallel to the +1 bp axis and the bulky substituents encroach the major groove. This common orientation would suggest that drug substitutions that impinge on the minor groove may be disfavored. Consistent with this possibility, substitutions on the camptothecins at positions 1 and 12 (see Fig. 1F) preclude topoisomerase I inhibition (13). In addition, minor groove substitutions with benzo[*a*]pyrene diol epoxide adducts on deoxyguanine *N2* prevent topoisomerase I from cleaving DNA when they occupy the topoisomerase I site in the DNA minor groove

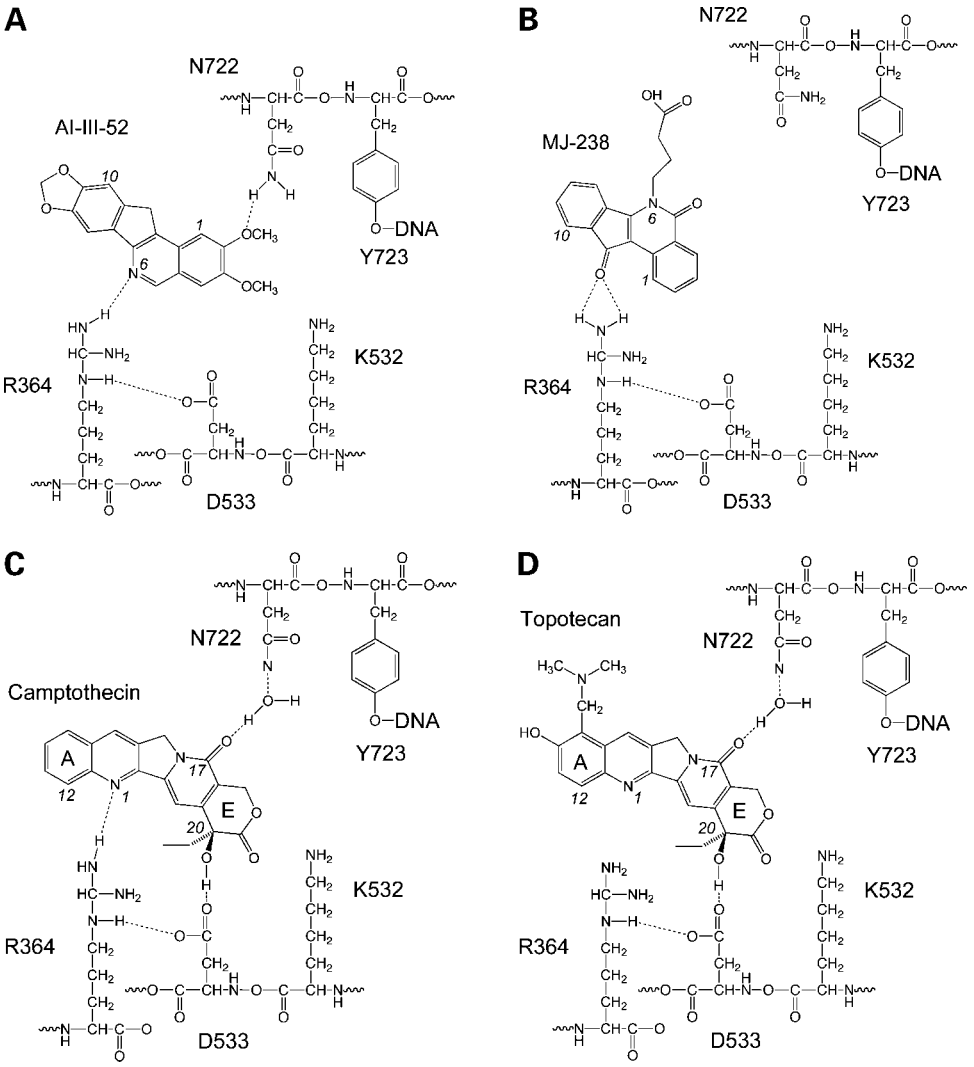


**Figure 4.** Hydrogen bond networks between drugs and topoisomerase I amino acid residues in the drug-topoisomerase I-DNA ternary complexes. **A,** AI-III-52 forms two direct hydrogen bonds with Asn$^{722}$ and Arg$^{364}$. **B,** MJ-238 forms only one hydrogen bond with Arg$^{364}$ (16). **C,** the natural camptothecin forms three hydrogen bonds with Asp$^{533}$, Asn$^{722}$, and Arg$^{364}$ (16). **D,** two hydrogen bonds have been reported for topotecan with Asn$^{722}$ and Arg$^{364}$ (15). The third hydrogen bond with Arg$^{364}$ has been proposed (see Discussion). Note that the water-mediated Asp$^{722}$ hydrogen bond is represented with the amino group of N722. It is also plausible to be with the carbonyl of N722 (data not shown).

(39). In contrast, substitutions toward the minor groove on indenoisoquinolines at position 11 (see Fig. 1F) result in more potent compounds for cytotoxicity and topoisomerase I inhibition (40–42). This suggests that these substitutions directly interact with topoisomerase I residues and strengthen the hydrogen bond network for these particular compounds.

### Indenoisoquinolines and Camptothecins Bind to Topoisomerase I by a Common Hydrogen Bond Network

A schematic representation of the hydrogen bond network for the two indenoisoquinolines and the two camptothecins is shown in Fig. 4. Two of the topoisomerase I catalytic residues are shown. Y723 forms the covalent bond with DNA. K532 serves a dual function. K532 forms a hydrogen bond on the minor groove side with the −1 base on the scissile strand (8, 15) and probably also functions as a general acid during cleavage to protonate the leaving 5′ oxygen (43). Three other topoisomerase I residues form hydrogen bonds with the intercalated drugs: N722, R364, and D533. None of these residues are essential for topoisomerase I catalytic activity. However, each of them has been implicated in resistance to camptothecins (4), indolocarbazoles (44), and indenoisoquinolines (23).

The norindenoisoquinoline AI-III-52 forms two hydrogen bonds, one with R364 and one with N722 (Fig. 4A). Only one hydrogen bond was detected for MJ-238 (16): with R364 (Fig. 4B). The weaker topoisomerase I inhibitory activity of MJ-238 compared with AI-III-52 (16, 24) can therefore be attributed to its reduced hydrogen bonding with topoisomerase I and to reduced stacking because of the smaller surface of its aromatic portion (Figs. 2 and 4, compare A and B).

The two camptothecins have a more similar H-bond network with the topoisomerase I-DNA complex than the indenoisoquinolines (Fig. 4). For camptothecin, three hydrogen bonds have been reported (Fig. 4C; ref. 16). Two are direct. One is between the camptothecin 20-hydroxy and D533, and the other between the camptothecin N1 and R364. The third H-bond has been proposed to be water mediated between the 17-carbonyl on the camptothecin D-ring and

N722 of topoisomerase I (16). For topotecan, only two of the three H-bonds (with D533 and N722) were initially reported (15) and are shown in Fig. 4D. Reexamination of the topotecan ternary structure reveals that the R364 side chain is also in close proximity with N1 of topotecan and is positioned for hydrogen bonding (15).

**Generalization of the Interfacial Inhibitor Concept**

To our knowledge, camptothecins were the first inhibitors hypothesized (14, 45) and shown (15) to bind at the ''interface of two macromolecules'' (topoisomerase I and its DNA substrate), as these macromolecules undergo a catalytic conformational change (the ''cleavage complex''; see Fig. 1A-C). This mechanism can be generalized as it also applies to three non-camptothecin inhibitors: two indenoisoquinolines and an indolocarbazole (see Fig. 2). The implications of these structures are twofold. First, they will aid for the rational synthesis of novel topoisomerase I inhibitors. However, the example of the two indenoisoquinolines that bind in flipped orientation (see Fig. 2A and B) shows the potential limitations of simple extrapolations from crystal structures, the need to correlate structural biology predictions with biological testing and ultimately additional atomic resolutions, and, hence, the need of an iterative process from chemistry to biology to structural biology, and again.

A second implication of the interfacial binding of topoisomerase I inhibitors is its apparent generality. The ''interfacial inhibition'' paradigm can be extended to a wide range of drugs and macromolecular targets (Table 2; refs. 26, 27). We therefore define ''interfacial inhibitors'' as drugs that bind at the interface of two (or more) macromolecules as the multimeric complex undergoes a structural transition. These multimeric complexes can present a drug binding site at their protein-protein interface as in the case of brefeldin A and tubulin inhibitors [colchicine, vinblastine, and paclitaxel (Taxol)] or a drug-binding site

**Table 2. Natural products that act as interfacial inhibitors**

| Drug | Origin | Substrate | Mechanism | References |
|---|---|---|---|---|
| Camptothecin | Chinese tree | Topoisomerase I-DNA complex | Stabilizes a kinetic intermediate of the DNA cleavage enzymic reaction | (15, 25, 47) |
| Brefeldin A | Ascomycetes | Arf-GDP-GEF complex | Stabilizes a kinetic protein-protein intermediate undergoing conformational changes | (48, 49) |
| Cyclosporine | Soil fungus | Cyclophilin/calcineurin | Hinders access to the active site of the protein phosphatase calcineurin by artificially creating a protein-protein interface | (50, 51) |
| FK506/tacrolimus | Actinomycetes (fungi-like bacteria) | FKBP/calcineurin | Idem | (52, 53) |
| Forskolin | Indian herb | Heterodimer of adenylyl cyclase | Activates the enzyme by stabilizing the heterodimer catalytic site in an active conformation | (54) |
| Fusicoccin | Fungus (plant parasite) | 14-3-3/ATPase complex | Overstabilizes a regulatory complex | (55) |
| Rapamycin | Soil bacteria | FKBP/FRAP | Promotes dimerization of FKBP12 with FRAP and inhibits mammalian target of rapamycin | (56) |
| Colchicine | Crocus | Tubulin heterodimer | Prevents tubulin polymerization by stabilizing a curved tubulin heterodimer | (57) |
| Vinblastine | *Vinca* | Tubulin heterodimer | Prevents tubulin polymerization by stabilizing a curved tubulin heterodimer | (58) |
| Taxol | Tree (*Taxus baccatus*) | β-Tubulin | Stabilizes microtubules | (59) |
| Epothilone A | Myxobacteria | β-Tubulin | Stabilizes microtubules | (60) |
| Kirromycin | Fungus | Antibiotics: bacterial ribosomes | Stabilization of translation elongation factors EF-Tu | (61, 62) |
| Fusidic acid | Fungus | Bacterial ribosome | Stabilization of translation factor EF-G | (61, 62) |
| Thiostrepton | *Streptomyces* | Bacterial ribosome | Prevents EF-G binding by altering the interface between ribosomal protein L11 and rRNA | (63) |
| Dexrazoxane (=ICRF-187) | Synthetic | Topoisomerase II-ATP complex | Stabilizes the closed topoisomerase II dimer | (64, 65) |
| α-Amanitin | ''Black cap'' mushroom | RNA polymerase II | Binds to Rpb1-Rpb2 interface and prevents polymerase II translocation | (66) |

at nucleic acid-protein interfaces as in the case of topoisomerase I inhibitors (present study), the RNA polymerase II inhibitor α-amanitin, and the antibiotic ribosome inhibitors [Table 2 (26, 27) and Fig. 3 (in a recent review; ref. 27)].

Interfacial inhibition is reversible and uncompetitive (26, 27). Interfacial inhibitors bind to and trap a catalytic intermediate of the macromolecular complex in a specific conformation (Fig. 5A). Interfacial inhibition represents a paradigm for ''uncompetitive inhibition'' (Fig. 5B and C: Lineweaver-Burke plot equations). The pharmacologic activity of interfacial inhibitors is due at least in part to the conversion of the trapped macromolecular intermediate into lethal lesions by other macromolecules that interact with the normally transient ternary drug-macromolecular complex. For instance, in the case of topoisomerase I inhibitors, the cleavage complexes are only lethal when they are converted into replication double-strand breaks by the collision of a DNA polymerase with a topoisomerase I cleavage complex reversibly trapped by the drug (46). This explains why the antiproliferative activity of topoisomerase I inhibitors increases with the levels of topoisomerase I. Conversely, a common resistance mechanism to topoisomerase I inhibitors is down-regulation of topoisomerase I (4). Hence, interfacial inhibitors differ from competitive inhibitors. Increasing drug target increases resistance to competitive inhibitors, whereas it sensitizes to interfacial inhibitors.

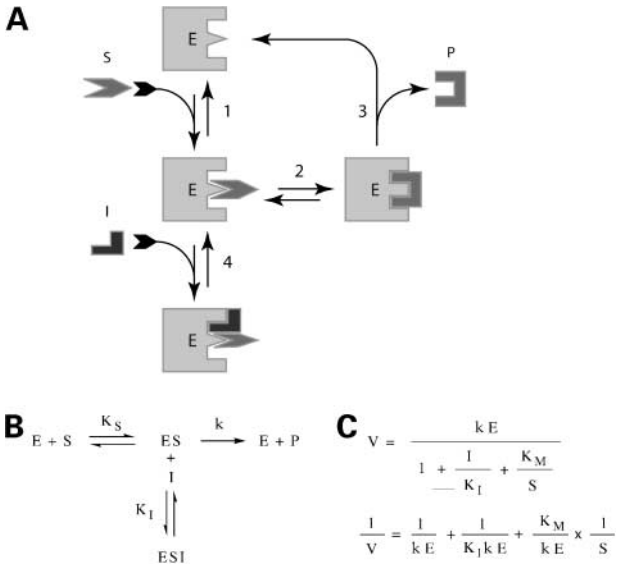


**Figure 5.** Generalization of the interfacial inhibitor paradigm. **A,** schematic cartoon representing the interfacial inhibition paradigm applied to an enzymatic system. *1,* a substrate (*S*) binds to an enzyme (*E*). *2,* the enzyme converts the substrate to product (*S*-to-*P*). *3,* P dissociates and the enzyme is regenerated for a new catalytic cycle. *4,* the interfacial inhibitor (*I*) binds at the enzyme-substrate ''interface'' and traps the enzyme-substrate complex, thereby reversibly preventing conversion of S-to-P. **B,** equilibrium representation of interfacial inhibition. $K_S$, substrate equilibrium dissociation constant; $K_I$, inhibitor equilibrium dissociation constant; *k,* catalytic constant. **C,** equations corresponding to uncompetitive scheme in **B**. *V,* reaction velocity; $K_M$, Michaelis-Menton equilibrium dissociation constant ($K_M = K_S$, when *k* is rate limiting).

The interfacial inhibitor paradigm has implications for drug discovery as interfacial inhibitors stabilize rather than inhibit the formation of macromolecular complexes. Assays should therefore be designed to look for drugs that stabilize rather than inhibit the formation of macromolecular complexes. Interfacial inhibitor screening using various methods to measure the binding of macromolecules has the potential to discover highly selective inhibitors for one particular receptor site and/or enzyme substrate.

## References


1. Lee MP, Brown SD, Hsieh T-S. DNA topoisomerase I is essential in *Drosophila melanogaster*. Proc Natl Acad Sci U S A 1993;90:6656 – 60.
2. Morham S, Kluckman KD, Voulomanos N, Smithies O. Targeted disruption of the mouse topoisomerase I gene by camptothecin selection. Mol Cell Biol 1996;16:6804 – 9.
3. Hsiang YH, Hertzberg R, Hecht S, Liu LF. Camptothecin induces protein-linked DNA breaks via mammalian DNA topoisomerase I. J Biol Chem 1985;260:14873 – 8.
4. Pommier Y, Pourquier P, Urasaki Y, Wu J, Laco G. Topoisomerase I inhibitors: selectivity and cellular resistance. Drug Resist Updat 1999;2:307 – 18.
5. Pommier Y, Pourquier P, Fan Y, Strumberg D. Mechanism of action of eukaryotic DNA topoisomerase I and drugs targeted to the enzyme. Biochim Biophys Acta 1998;1400:83 – 105.
6. Champoux JJ. DNA TOPOISOMERASES: structure, function, and mechanism. Annu Rev Biochem 2001;70:369 – 413.
7. Wang JC. Cellular roles of DNA topoisomerases: a molecular perspective. Nat Rev Mol Cell Biol 2002;3:430 – 40.
8. Stewart L, Redinbo MR, Qiu X, Hol WGJ, Champoux JJ. A model for the mechanism of human topoisomerase I. Science 1998;279:1534 – 41.
9. Wall ME, Wani MC. Camptothecin and Taxol: discovery to clinic—thirteenth Bruce F. Cain Memorial Award lecture. Cancer Res 1995;55:753 – 60.
10. Eng WK, Faucette L, Johnson RK, Sternglanz R. Evidence that DNA topoisomerase I is necessary for the cytotoxic effects of camptothecin. Mol Pharmacol 1988;34:755 – 60.
11. Nitiss J, Wang JC. DNA topoisomerase-targeting antitumor drugs can be studied in yeast. Proc Natl Acad Sci U S A 1988;85:7501 – 5.
12. Bjornsti M-A, Benedetti P, Viglianti GA, Wang JC. Expression of human DNA topoisomerase I in yeast cells lacking yeast DNA topoisomerase I: restoration of sensitivity of the cells to the antitumor drug camptothecin. Cancer Res 1989;49:6318 – 23.
13. Jaxel C, Kohn KW, Wani MC, Wall ME, Pommier Y. Structure-activity study of the actions of camptothecin derivatives on mammalian topoisomerase I: evidence for a specific receptor site and a relation to antitumor activity. Cancer Res 1989;49:1465 – 9.
14. Jaxel C, Capranico G, Kerrigan D, Kohn KW, Pommier Y. Effect of local DNA sequence on topoisomerase I cleavage in the presence or absence of camptothecin. J Biol Chem 1991;266:20418 – 23.
15. Staker BL, Hjerrild K, Feese MD, Behnke CA, Burgin AB, Jr, Stewart L. The mechanism of topoisomerase I poisoning by a camptothecin analog. Proc Natl Acad Sci U S A 2002;99:15387 – 92.
16. Staker BL, Feese MD, Cushman M, et al. Structures of three classes of anticancer agents bound to the human topoisomerase I-DNA covalent complex. J Med Chem 2005;48:2336 – 45.
17. Meng L-H, Liao Z-H, Pommier Y. Non-camptothecin DNA topoisomerase I inhibitors in cancer chemotherapy. Curr Top Med Chem 2003;3:305 – 20.
18. Pizzolato JF, Saltz LB. The camptothecins. Lancet 2003;361:2235 – 42.
19. Thomas CJ, Rahier NJ, Hecht SM. Camptothecin: current perspectives. Bioorg Med Chem 2004;12:1585 – 604.
20. Burke TG, Mi ZM. The structural basis of camptothecin interactions with human serum albumin: impact on drug stability. J Med Chem 1994;37:40 – 6.
21. Brangi M, Litman T, Ciotti M, et al. Camptothecin resistance: role of the ATP binding cassette (ABC) half-transporter, mitoxantrone-resistance (MXR), and potential for glucuronidation in MXR-expressing cells. Cancer Res 1999;59:5938 – 46.

**22.** Kohlhagen G, Paull K, Cushman M, Nagafufuji P, Pommier Y. Protein-linked DNA strand breaks induced by NSC 314622, a non-camptothecin topoisomerase I poison. Mol Pharmacol 1998;54:50 – 8.

**23.** Antony S, Jayaraman M, Laco G, et al. Differential induction of topoisomerase I-DNA cleavage complexes by the indenoisoquinoline MJ-III-65 (NSC 706744) and camptothecin: base sequence analysis and activity against camptothecin-resistant topoisomerases I. Cancer Res 2003;63:7428 – 35.

**24.** Ioanoviciu A, Antony S, Pommier Y, Staker BL, Stewart L, Cushman M. Synthesis and mechanism of action studies of a series of norindenoisoquinoline topoisomerase I poisons reveal an inhibitor with a flipped orientation in the ternary DNA-enzyme-inhibitor complex as determined by X-ray crystallographic analysis. J Med Chem 2005;48:4803 – 14.

**25.** Chrencik JE, Staker BL, Burgin AB, et al. Mechanisms of camptothecin resistance by human topoisomerase I mutations. J Mol Biol 2004;339:773 – 84.

**26.** Pommier Y, Cherfils J. Interfacial protein inhibition: a nature's paradigm for drug discovery. Trends Pharmacol Sci 2005;28:136 – 45.

**27.** Pommier Y, Marchand C. Interfacial inhibitors of protein-nucleic acid interactions. Curr Med Chem Anti-Canc Agents 2005;5:421 – 9.

**28.** Stewart L, Ireton G, Parker L, Madden KR, Champoux JJ. Biochemical and Biophysical analyses of recombinant forms of human topoisomerase I. J Biol Chem 1996;271:7593 – 601.

**29.** Navaza J. Implementation of molecular replacement in AMoRe. Acta Crystallogr D Biol Crystallogr 2001;57:1367 – 72.

**30.** Brunger AT, Adams PD, Clore GM, et al. Crystallography & NMR system: a new software suite for macromolecular structure determination. Acta Crystallogr D Biol Crystallogr 1998;54:905 – 21.

**31.** Murshudov GN, Vagin AA, Dodson EJ. Refinement of macromolecular structures by the maximum-likelihood method. Acta Crystallogr D Biol Crystallogr 1997;53:240 – 55.

**32.** McRee DE. XtalView/Xfit—a versatile program for manipulating atomic coordinates and electron density. J Struct Biol 1999;125:156 – 65.

**33.** Oldfield TJ. X-LIGAND: an application for the automated addition of flexible ligands into electron density. Acta Crystallogr D Biol Crystallogr 2001;57:696 – 705.

**34.** Redinbo MR, Stewart L, Kuhn P, Champoux JJ, Hol WGJ. Crystal structure of human topoisomerase I in covalent and noncovalent complexes with DNA. Science 1998;279:1504 – 13.

**35.** Carey JF, Schultz SJ, Sisson L, Fazzio TG, Champoux JJ. DNA relaxation by human topoisomerase I occurs in the closed clamp conformation of the protein. Proc Natl Acad Sci U S A 2003;100:5640 – 5.

**36.** Woo MH, Losasso C, Guo H, Pattarello L, Benedetti P, Bjornsti MA. Locking the DNA topoisomerase I protein clamp inhibits DNA rotation and induces cell lethality. Proc Natl Acad Sci U S A 2003;100:13767 – 72.

**37.** Stewart L, Ireton G, Champoux JJ. The domain organization of human topoisomerase I. J Biol Chem 1996;271:7602 – 8.

**38.** Xiao X, Cushman M. Effect of E-ring modifications in camptothecin on topoisomerase I inhibition: a quantum mechanics treatment. J Org Chem 2005;70:9584 – 7.

**39.** Pommier Y, Kohlhagen G, Laco GS, Kroth H, Sayer JM, Jerina DM. Different effects on human topoisomerase I by minor groove and intercalated deoxyguanosine adducts derived from two polycyclic aromatic hydrocarbon diol epoxides at or near a normal cleavage site. J Biol Chem 2002;277:13666 – 72.

**40.** Fox BM, Xiao X, Antony S, et al. Design, synthesis, and biological evaluation of cytotoxic 11-alkenylindenoisoquinoline topoisomerase I inhibitors and indenoisoquinoline-camptothecin hybrids. J Med Chem 2003;46:3275 – 82.

**41.** Xiao X, Antony S, Kohlhagen G, Pommier Y, Cushman M. Novel autoxidative cleavage reaction of 9-fluoredenes discovered during synthesis of a potential DNA-threading indenoisoquinoline. J Org Chem 2004;69:7495 – 501.

**42.** Xiao X, Antony S, Kohlhagen G, Pommier Y, Cushman M. Design, synthesis, and biological evaluation of cytotoxic 11-aminoalkenylindenoisoquinoline and 11-diaminoalkenylindenoisoquinoline topoisomerase I inhibitors. Bioorg Med Chem 2004;12:5147 – 60.

**43.** Interthal H, Quigley PM, Hol WG, Champoux JJ. The role of lysine 532 in the catalytic mechanism of human topoisomerase I. J Biol Chem 2004;279:2984 – 92.

**44.** Urasaki Y, Laco G, Takebayashi Y, Bailly C, Kohlhagen G, Pommier Y. Use of camptothecin-resistant mammalian cell lines to evaluate the role of topoisomerase I in the antiproliferative activity of the indolocarbazole, NB-506, and its topoisomerase I binding site. Cancer Res 2001;61:504 – 8.

**45.** Capranico G, Kohn KW, Pommier Y. Local sequence requirements for DNA cleavage by mammalian topoisomerase II in the presence of doxorubicin. Nucleic Acids Res 1990;18:6611 – 9.

**46.** Strumberg D, Pilon AA, Smith M, Hickey R, Malkas L, Pommier Y. Conversion of topoisomerase I cleavage complexes on the leading strand of ribosomal DNA into 5′-phosphorylated DNA double-strand breaks by replication runoff. Mol Cell Biol 2000;20:3977 – 87.

**47.** Staker BL, Feese MD, Cushman M, et al. Structure of three classes of anticancer agents bound to the human topoisomerase I-DNA covalent complex. J Med Chem 2005;48:2336 – 45.

**48.** Renault L, Guibert B, Cherfils J. Structural snapshots of the mechanism and inhibition of a guanine nucleotide exchange factor. Nature 2003;426:525 – 30.

**49.** Mossessova E, Corpina RA, Goldberg J. Crystal structure of ARF1*Sec7 complexed with brefeldin A and its implications for the guanine nucleotide exchange mechanism. Mol Cell 2003;12:1403 – 11.

**50.** Jin L, Harrison SC. Crystal structure of human calcineurin complexed with cyclosporin A and human cyclophilin. Proc Natl Acad Sci U S A 2002;99:13522 – 6.

**51.** Huai Q, Kim HY, Liu Y, et al. Crystal structure of calcineurin-cyclophilin-cyclosporin shows common but distinct recognition of immunophilin-drug complexes. Proc Natl Acad Sci U S A 2002;99:12037 – 42.

**52.** Kissinger CR, Parge HE, Knighton DR, et al. Crystal structures of human calcineurin and the human FKBP12-506-calcineurin complex. Nature 1995;378:641 – 4.

**53.** Griffith JP, Kim JL, Kim EE, et al. X-ray structure of calcineurin inhibited by the immunophilin-immunosuppressant FKBP12-506 complex. Cell 1995;82:507 – 22.

**54.** Tesmer JJ, Sunahara RK, Gilman AG, Sprang SR. Crystal structure of the catalytic domains of adenylyl cyclase in a complex with Gsα. GTPγS. Science 1997;278:1907 – 16.

**55.** Wurtele M, Jelich-Ottmann C, Wittinghofer A, Oecking C. Structural view of a fungal toxin acting on a 14-3-3 regulatory complex. EMBO J 2003;22:987 – 94.

**56.** Choi J, Chen J, Schreiber SL, Clardy J. Structure of the FKBP12-rapamycin complex interacting with the binding domain of human FRAP. Science 1996;273:239 – 42.

**57.** Ravelli RB, Gigant B, Curmi PA, et al. Insight into tubulin regulation from a complex with colchicine and a stathmin-like domain. Nature 2004;428:198 – 202.

**58.** Gigant B, Wang C, Ravelli RB, et al. Structural basis for the regulation of tubulin by vinblastine. Nature 2005;435:519 – 22.

**59.** Snyder JP, Nettles JH, Cornett B, Downing KH, Nogales E. The binding conformation of Taxol in β-tubulin: a model based on electron crystallographic density. Proc Natl Acad Sci U S A 2001;98:5312 – 6.

**60.** Nettles JH, Li H, Cornett B, Krahn JM, Snyder JP, Downing KH. The binding mode of epothilone A on α,β-tubulin by electron crystallography. Science 2004;305:866 – 9.

**61.** Agrawal RK, Frank J. Structural studies of the translational apparatus. Curr Opin Struct Biol 1999;9:215 – 21.

**62.** Laurberg M, Kristensen O, Martemyanov K, et al. Structure of a mutant EF-G reveals domain III and possibly the fusidic acid binding site. J Mol Biol 2000;303:593 – 603.

**63.** Bowen WS, Van Dyke N, Murgola EJ, Lodmell JS, Hill WE. Interaction of thiostrepton and elongation factor-G with the ribosomal protein L11-binding domain. J Biol Chem 2005;280:2934 – 43. Epub 2004 Oct 18.

**64.** Roca J, Ishida R, Berger JM, Andoh T, Wang JC. Antitumor bisdioxopiperazines inhibit yeast DNA topoisomerase II by trapping the enzyme in the form of a closed protein clamp. Proc Natl Acad Sci U S A 1994;91:1781 – 5.

**65.** Classen S, Olland S, Berger JM. Structure of the topoisomerase II ATPase region and its mechanism of inhibition by the chemotherapeutic agent ICRF-187. Proc Natl Acad Sci U S A 2003;100:10629 – 34.

**66.** Bushnell DA, Cramer P, Kornberg RD. Structural basis of transcription: α-amanitin-RNA polymerase II cocrystal at 2.8 A resolution. Proc Natl Acad Sci U S A 2002;99:1218 – 22.

Molecular Cancer Therapeutics

# A novel norindenoisoquinoline structure reveals a common interfacial inhibitor paradigm for ternary trapping of the topoisomerase I-DNA covalent complex

Christophe Marchand, Smitha Antony, Kurt W. Kohn, et al.

*Mol Cancer Ther* 2006;5:287-295.